The relationship between interlayer spacing and magnetic ordering in gadolinium

2000 J. Phys.: Condens. Matter 12 10441

(http://iopscience.iop.org/0953-8984/12/50/307)

J. Phys.: Condens. Matter **12** (2000) 10441–10456. Printed in the UK PII: S0953-8984(00)13659-8

The relationship between interlayer spacing and magnetic ordering in gadolinium

A C Jenkins†, W M Temmerman†, R Ahuja‡, O Eriksson‡, B Johansson‡ and J Wills§

† Daresbury Laboratory, Daresbury, Cheshire WA4 4AD, UK
‡ Condensed Matter Theory Group, Department of Physics, Uppsala University, BOX 530, S-751 21, Uppsala, Sweden
§ Theoretical Division, Los Alamos National Laboratory, Los Alamos, NM 87545, USA

Received 3 May 2000, in final form 3 October 2000

Abstract. We report on the application of the local spin-density approximation (LSDA) and the generalized gradient approximation of Perdew, Burke and Ernzerhof (PBE) within the linear muffin-tin orbital method in both the atomic sphere approximation (LMTO-ASA) and in the full-potential (FP-LMTO) method to the description of the magnetic coupling within bulk Gd. Using the LMTO-ASA approach to the band-structure problem it is found that, at the experimental lattice parameters, the PBE approximation predicts the experimentally observed ferromagnetic (FM) ground state whereas the LSDA does not. Moreover the nature of the magnetic coupling between successive layers is found to be dependent on the interlayer separation—in particular a reduction of the interlayer spacing will lead to an increased tendency towards FM coupling between successive layers and, conversely, increase of the interlayer spacing will lead to antiferromagnetic (AFM) coupling between layers being energetically favourable. A similar interdependence between the interlayer spacing and the magnetic coupling is also observed from calculations using the FP-LMTO method. These observations are used to analyse the nature of the magnetic coupling of the Gd(0001) surface to the underlying FM bulk.

1. Introduction

1.1. Bulk

The highly localized nature of the 4f electrons in Gd, combined with anticipation that relativistic and exchange effects play a significant role in the determination of the electronic structure, make this metal a particularly good test case for the applicability of density functional theory (DFT) methods to rare-earth systems. Indeed it has been reported that use of the local spin-density approximation (LSDA) within the linear muffin-tin orbital method in the atomic sphere approximation (LMTO-ASA) framework will predict an antiferromagnetic (AFM) ground state for bulk hcp rather than the experimentally observed ferromagnetic (FM) ground state [1, 2]. This has been attributed to the fact that the LSDA has a tendency to overestimate the extent of the itinerancy of the 4f electrons which may, as a consequence, lead to an overestimation of the strength of the 4f bonding [3–5]. A further example of the inadequacy of the LSDA concerns the magnetic ground state of bulk Fe—the ground-state structure is predicted to be non-magnetic fcc rather than the experimentally observed FM bcc [6]. Use of a generalized gradient approximation (GGA) will introduce some inhomogeneity into the solution of the DFT band-structure problem. This usually has the effect of inducing a small increase in

0953-8984/00/5010441+16$30.00

the equilibrium volume and a small gain in the magnetic energy. Consequently use of a GGA instead of the LSDA may lead to a change in the preferred magnetic coupling within the material and the prediction of ground-state properties that are in agreement with those observed experimentally; for example, the correct magnetic ground states are predicted for bulk Gd [1, 2] and bulk Fe [7].

The correct treatment of these Gd 4f electrons has presented a dilemma: is it better to treat them as valence or core electrons [2, 5, 8–11]? The first approach seems to be most suitable as the seven occupied spin-up 4f states lie below the Fermi energy and the unoccupied spin-down 4f states above the Fermi energy. However, treating the 4f electrons as core electrons may also be suitable; this is compatible with the localized nature of these electrons. A study of Gd which addressed this question has indicated that, within a fully relativistic full-potential linear muffin-tin orbital (FP-LMTO) method framework, a FM ground state may be obtained for bulk hcp Gd if the 4f electrons are treated as core electrons with an AFM ground state predicted if the 4f electrons are treated with the valence band—regardless of whether a LSDA or GGA functional is used [11]. Such conclusions are contrary to the results presented by Heinemann and Temmerman [1, 2]—for which the 4f electrons were treated within the valence band. The apparent disparities between the conclusions reached by Eriksson and Temmerman [11] and Heinemann and Temmerman [1, 2] could be due to the fact that in the former approach a FP description of the potential is used whereas in the latter the potential is described using the ASA.

1.2. Surface

The nature of the magnetic coupling of the Gd(0001) surface to the underlying FM bulk has also been the focal point of much discussion during the past fifteen years. Indeed there have been many conflicts of opinion due to variations in the reliability and interpretation of data, in both experimental and theoretical arenas, concerning the direction and magnitude of relaxation of the gadolinium (0001) surface and the nature of the magnetic coupling of this surface to the underlying FM bulk [12, 13].

An early theoretical study of the gadolinium (0001) surface, using the all-electron local density full-potential LAPW method, concluded that the surface atoms occupied the hcp sites within the lattice frame, the surface layer relaxed outwards by about 6% and there is AFM coupling between the surface and the underlying FM bulk [10, 14]. Interpretation of LEED diffraction data also suggested that the surface atoms occupied the hcp lattice sites and, although it could not indicate the nature of the magnetic coupling at the surface, it also suggested that the surface layer relaxed inwards by 3% [15]. Photoemission data seemed to confirm that the magnetic coupling between the surface and the underlying bulk was AFM [16]. However, one must note that the reliability of this particular set of photoemission data has been questioned [17].

Later experimental data confirmed that the gadolinium atom does indeed occupy the hcp lattice site [17–19]. But, in contrast to earlier experimental and theoretical work, interpretation of this data indicated that the coupling between the surface and subsurface layer was FM and, in agreement with the early LEED study [15], the surface layer contracts by about 3%. All three conclusions reached from these later experimental studies have been successfully modelled theoretically [11, 20].

Recent experimental [21] and theoretical [22] work has indicated that the easy axis of magnetization of bulk gadolinium is temperature dependent and the magnetic coupling between the surface and the underlying bulk is predominantly FM with a perpendicular surface magnetization component. However, for simplicity, such non-collinear effects will

be neglected within this work and the desired layerwise magnetic coupling, both for the bulk and at the (0001) surface, will be taken to be FM.

A further point of controversy, addressed in the last few years, is the temperature dependence of the exchange splitting of the (0001) surface state. From analysis of spin-polarized photoemission data, a distinct difference in the behaviour of the exchange splitting for the bulk and surface has been observed [23]. In particular, while Stoner-like behaviour is observed as a function of temperature for the bulk material, the spin-up and spin-down channels of the surface state hybridize as a consequence of fluctuating local moments. This qualitatively different behaviour of the temperature dependence of the exchange splitting at the surface and in the bulk has been interpreted as originating from the idea that the f electrons are more localized at the surface than in the bulk [23]. In direct contrast to this, from angle-resolved photoemission and inverse photoemission studies, a Stoner-like temperature variation of the surface-state exchange splitting has also been observed [24]. Subsequent spin-resolved inverse photoemission experiments confirmed that there is Stoner-like behaviour at the surface [25] but, although both Li *et al* [23] and Weschke *et al* [24] observed an enhancement of the surface Curie temperature, there was no indication of exceptional behaviour of the magnetic properties at the surface. Consequently in this theoretical study of the magnetism of the Gd(0001) surface it will be assumed that there is no such enhancement of the Curie temperature at the surface and the magnetic ordering within the surface does not differ from that of the bulk.

The organization of the paper is as follows. In section 2 details of the LMTO-ASA and FP-LMTO method, used to solve the band-structure problem, are discussed. In section 3 a study of the interlayer magnetic coupling for bulk Gd and the Gd(0001) surface is presented and in section 4 a brief summary of the major points is given.

2. Methodology

2.1. LMTO set-up

The LMTO methods used in this study are the self-consistent semi-relativistic LMTO-ASA method, as implemented within the Stuttgart LMTO46 code [26], and the self-consistent fully relativistic FP-LMTO method, as implemented within the Wills code [27, 28]. Both of these density functional theory (DFT) methods were applied, using the LSDA (von Barth–Hedin [29]) and Perdew–Burke–Ernzerhof (PBE) [30] functionals, to the description of the electronic structure of bulk hcp gadolinium and the LMTO-ASA method is also applied to a description of the magnetic coupling at the Gd(0001) surface using supercell techniques. Throughout both sets of calculations the 4f electrons were treated as itinerant band states—although one may recall that this results in the prediction of an AFM rather than a FM ground state for bulk Gd using the Wills FP-LMTO method [11] while a FM ground state is predicted using fully relativistic LMTO-ASA techniques [1, 2].

In the LMTO-ASA calculations we make the size of the muffin tins equal to the volume of those overlapping spheres whose volume is identical to that of the unit cell. Throughout all of the calculations using this approach to the description of the potential we have used a basis set of muffin-tin orbitals with $l_{max} = 3$ and a single energy panel. All 6s, 6p, 5d and 4f electrons were treated within this basis as 'low' partial wavefunctions and all other electrons were treated within the core. Typically about 800 k-points were required to ensure that the total energy was converged, with respect to the number of k-points, to an accuracy of about 0.5 mRyd per atom.

In the FP-LMTO calculations the shape of the charge density and potential inside the muffin tins and in the interstitial region is not restricted. The basis set, charge density and

potential are expanded using spherical harmonics, with $l_{max} = 8$, within the *non-overlapping* muffin-tin spheres and using a Fourier series in the interstitial region. Our basis set comprised linear muffin-tin orbitals in which the 6s, 6p, 5p, 5d and 4f electrons were treated within the valence band using a double basis in order to take account of the dispersion of the 5p states. The integration over the BZ was done using special-k-point sampling [31,32] and a Gaussian smearing of 20 mRyd. To achieve k-point convergence to within 0.5 mRyd per atom we were obliged to use 75 k-points in the $1/12$ of the irreducible wedge of the BZ.

It may be noted that calculations of the electronic structure of bulk hcp Gd were also done using the PW91 [33,34] functional. The data obtained using this functional were found to be qualitatively similar to those predicted using the PBE one—using both ASA and FP treatments of the potential. However, it was found that, using the ASA approach, the PBE functional makes the self-consistency cycles much more stable and so will reduce the number of iterations required for convergence by about 50% when compared to those done using the PW91 functional. Consequently preference will be given to the implementation of the PBE functional in our calculations and all discussion henceforth will focus primarily on the data obtained using the LSDA and PBE functionals.

2.2. Physical set-up

Bulk Gd is hcp structured with two atoms per unit cell for both the FM and AFM_I structures. The AFM_{II} structure requires the use of an orthorhombic cell with four atoms per unit cell. In all magnetic structures it is assumed that the magnetic moment on each atom site is collinear with the c-axis as this is the easy axis of magnetization at room temperature. For the FM structure all atoms have magnetic moments parallel to the c-axis as illustrated in figure 1(a). The AFM_I and AFM_{II} structures are constructed, with reference to the ferromagnetic structure, by flipping over the magnetic moment on alternate planes in either the (001) direction, figure 1(b), or the (111) direction, figure 1(c), respectively.

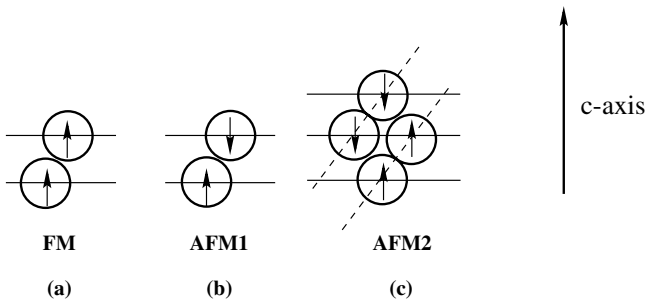

Figure 1. An illustration of the orientation of the magnetic moments within a FM (a), AFM_I (b) or AFM_{II} (c) structure. Here the solid and dashed lines show the positions of the (001) and (111) layers respectively.

The total energy and magnetic moment per atom for FM and AFM ordered hcp structured Gd were calculated as functions of volume using both FP-LMTO and LMTO-ASA approaches. Firstly a fixed c/a, corresponding to $c_0 = 5.7480$ Å and $a_0 = 3.622$ Å as given by Wu *et al* [10], was used to discover which method and which functional were able to correctly predict the magnetic ground state and then, using a fixed volume, corresponding to $V_0 = (\sqrt{3}/2)a_0^3 c_0/a_0 = 32.65$ Å^3, the c/a ratio was varied to gain an understanding of the relationship between the interlayer spacing and the magnetic coupling. This could then be related to the magnetic coupling at the Gd(0001) surface.

A description of the magnetic coupling at the Gd(0001) surface was obtained using supercell techniques, in which a supercell consisting of a five-layer slab of Gd interspersed with three layers of 'empty spheres' was constructed. The atoms within the Gd surface layer are assumed to occupy the hcp lattice sites with the magnetic moment on these surface atoms either parallel or antiparallel to the underlying FM bulk as illustrated in figures 2(a) and 2(b) respectively. This surface layer is relaxed, both outwards and inwards, with the positions of all other layers within the supercell remaining fixed. The total energy of the supercell for various relaxations was calculated for both FM and AFM coupling of the surface to the underlying bulk using LMTO-ASA methods.

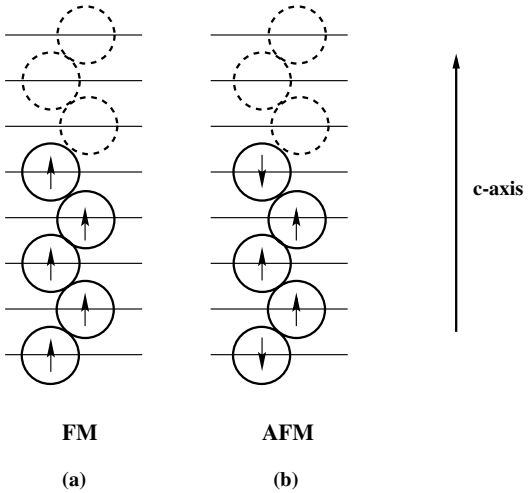

Figure 2. A schematic picture of the construction of a hcp supercell, consisting of five layers of Gd and three layers of empty spheres, with FM (a) or AFM (b) coupling of the (0001) surface to the underlying FM bulk.

3. Interlayer coupling

3.1. At the experimental c/a

The energy–volume curves for FM, AFM_I and AFM_{II} structured hcp Gd, for a fixed c/a ratio of $c_0/a_0 = 1.587$, were calculated using the LSDA and the PBE functionals within the LMTO-ASA and are presented in figures 3 and 4 respectively. From these figures it is evident that, at the experimental lattice parameters, the PBE functional predicts the experimentally observed FM ground state whereas the LSDA functional predicts that the AFM_I structure is energetically favourable. This change in preferred magnetic ordering is a direct consequence of the increase in equilibrium volume coupled with the gain in magnetic energy induced by the introduction of some inhomogeneity into the description of the exchange–correlation energy by the use of the GGA. Moreover, for the FM structure, the PBE functional gives an equilibrium volume that is $1.05V_0$ whereas the LSDA functional gives one that is far too small ($0.88V_0$). This increase in lattice parameter is a common trend in calculations done using a GGA when compared to LSDA calculations and has been attributed to the redistribution of charge due to the stronger exchange repulsion in some parts of space [2]. Consequently it may be concluded that a better description of the magnetic ordering in bulk hcp Gd can be obtained using the PBE functional rather than the LSDA one.

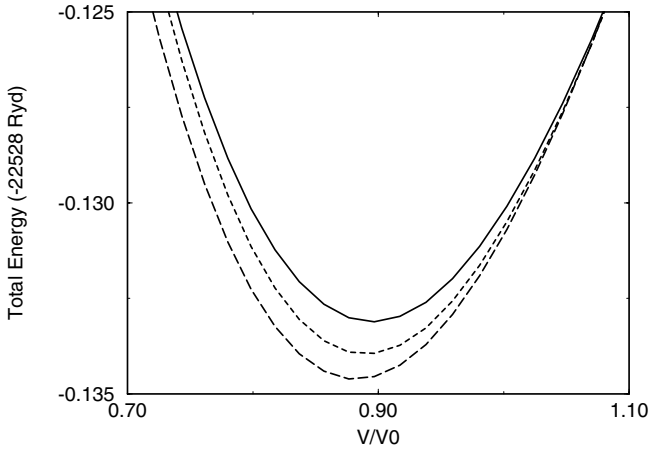

Figure 3. The energy–volume curve for hcp gadolinium calculated using the LSDA functional and $c/a = c_0/a_0$. Here the results for the ferromagnetic (solid line) and antiferromagnetic (AFM_I, dashed line; AFM_{II}, dotted line) structures are presented. V_0 represents the experimental equilibrium volume.

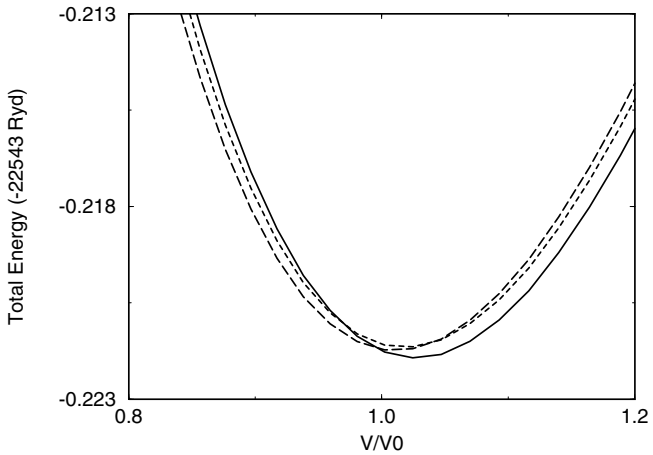

Figure 4. The energy–volume curve for hcp gadolinium calculated using the PBE functional and $c/a = c_0/a_0$. Here the results for the ferromagnetic (solid line) and antiferromagnetic (AFM_I, dashed line; AFM_{II}, dotted line) structures are presented. V_0 represents the experimental equilibrium volume.

Comparison of these semi-relativistic LMTO-ASA calculations with fully relativistic LMTO-ASA calculations, by Heinemann and Temmerman [1,2], confirm that a GGA is indeed required to obtain the correct magnetic ground state for bulk hcp Gd. This is despite the slightly different treatments of the 5p electrons—in both [1] and [2] two-panel calculations were done, so the 5p semi-core electrons were allowed to relax [35], and in the LMTO-ASA calculations presented here one energy panel was used and the 5p electrons are treated within the core. It may also be noted that different GGAs were used—LMH [36, 37] in [1, 2] and PW91 [33] or the PBE functional [30] in this work. Therefore one may suggest that the inclusion of spin–orbit coupling, the relaxation of the 5p electrons and the choice of GGA do not play a significant role in the determination of the magnetic ground state of bulk hcp Gd using the

LMTO-ASA. However, the treatment of the 5p electrons does have some influence on the equilibrium lattice parameters—namely that the LSDA gives an equilibrium volume that is in excellent agreement with experiment ($1.05V_0$) or far too small ($0.88V_0$) if these electrons are treated as semi-core or core respectively. Introduction of a GGA will shift this equilibrium value by +12%, regardless of the details of the calculation, thus enabling one to obtain a FM ground state with an equilibrium volume which is in excellent agreement with experiment if these 5p electrons are treated within the core.

The total energy as a function of V/V_0, calculated using FP-LMTO methods, is presented in figures 5 and 6 using the LSDA and PBE functionals respectively. From both figures it

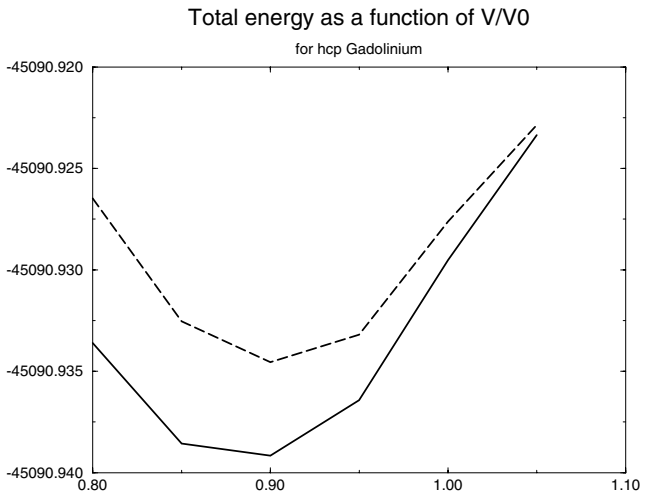

Figure 5. The energy–volume curve calculated using the LSDA within the FP-LMTO method for AFM structure (full line) and FM structure (dashed line). The experimental c/a ratio was used and V_0 represents the experimental equilibrium volume.

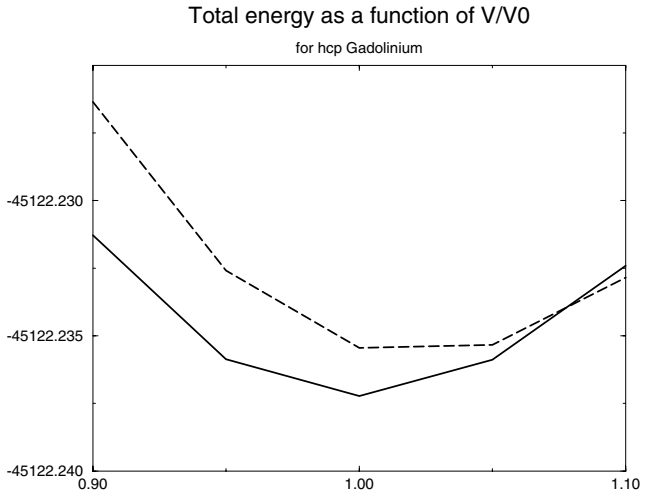

Figure 6. The energy–volume curve calculated using the PBE functional within the FP-LMTO method for AFM structure (full line) and FM structure (dashed line). The experimental c/a ratio was used and V_0 represents the experimental equilibrium volume.

is apparent that the energetically favoured structure is that of an AFM—regardless of which functional is used within our calculation. Indeed this is the same conclusion as that reached by reference [11] in which the LSDA and PW91 functionals were used within this FP-LMTO method. Consequently again one can say that the PW91 and PBE functionals give qualitatively the same results. However, it is found that the difference between the FM and AFM_I structure is smaller in the PW91 calculations than the PBE ones—this will be discussed further in the next section.

From the FP-LMTO calculations the equilibrium volume of the FM structure is found to be $0.84V_0$ and $1.03V_0$ using the LSDA and PBE functional respectively. Consequently one can state that the use of the PBE functional within either LMTO method will have the effect of invoking a similar proportional increase in equilibrium volume compared to that predicted using the LSDA. It must also be noted that, again in agreement with the trends predicted using LMTO-ASA methods, at a sufficiently large volume compression there is a tendency towards AFM behaviour being energetically favourable and, conversely, FM behaviour is energetically favoured under volume expansion.

The highly localized 4f electrons in gadolinium metal induce a large and parallel spin polarization of the valence 5d and 6s electrons. Consequently the magnetic moment per atom is dominated by 7 μ_B from the 4f electrons with a smaller contribution, experimentally determined to be 0.63 μ_B [38], from the other valence electrons. The total magnetic moment and partial contributions to the magnetic moment per atomic site calculated at the experimental lattice parameter using the LMTO-ASA and FP-LMTO methods are presented in tables 1 and 2 respectively. Examination of the partial contributions to the magnetic moment indicate that for LMTO-ASA calculations in the FM structure the total induced conduction moment is slightly smaller than the experimental value, 0.55 μ_B or 0.59 μ_B calculated using the LSDA or PBE

Table 1. Magnetic moments for bulk hcp Gd calculated for the experimental lattice parameters. The calculations were made treating the 4f as band and 5p as core electrons using the LSDA and PBE functionals. Here we present the total magnetic moment for AFM_I, AFM_{II} and FM ordering.

Structure	Functional	s	p	d	f	Moment
FM	LSDA	0.020	0.124	0.403	6.879	7.427
	PBE	0.023	0.140	0.430	6.910	7.503
AFM_I	LSDA	0.031	0.040	0.341	6.833	7.244
	PBE	0.036	0.050	0.370	6.860	7.317
AFM_{II}	LSDA	0.027	0.049	0.345	6.834	7.257
	PBE	0.033	0.061	0.382	6.862	7.339

Table 2. s, p, d, f, total muffin-tin (tot from mt), interstitial (int) and total (tot) contributions to total magnetic moments for AFM and FM structures at the experimental lattice parameter—calculated using the FP-LMTO method.

LSDA	s	p	d	f	tot from mt	int	tot
FM	0.015	0.069	0.339	6.842	7.267	0.284	7.550
AFM	0.027	0.038	0.313	6.826	7.204	0	7.204
PBE	s	p	d	f	tot from mt	int	tot
FM	0.015	0.070	0.338	6.853	7.276	0.288	7.565
AFM	0.026	0.039	0.309	6.836	7.210	0	7.210

functional respectively, and the contribution from the 4f electrons is about 0.1 μ_B too small. Similarly from the FP-LMTO calculations the total induced magnetic moment in the muffin-tin region is 0.42 μ_B with a contribution from the 4f electrons of 6.84 μ_B and an additional contribution, due to the interstitial region, of 0.28 μ_B per atom for the FM structure. It may be noted that this contribution to the total magnetic moment per atom in the FM structure from the interstitial region is comparable to the contribution made by the d electrons, and inclusion of this 'interstitial' term results in the magnetic moment per site being in better agreement with experiment than if the LMTO-ASA method was used. Consequently it is evident that the correct treatment of the magnetism within the interstitial region is important if one wishes to be able to obtain a good description of the magnetism within Gd. Both LMTO methods used in this study make some assumption regarding the interstitial region. In the ASA approach one 'blows up' the muffin-tin spheres such that the total volume of the spheres is equivalent to the volume of the unit cell and so one has errors due to the overlap of these spheres. This overlap is typically of the order 9% between atoms sitting in the same layer and 12% between atoms on different layers. In the FP-LMTO method the muffin-tin spheres do not overlap and there are no restrictions on the shape of the potential, inside or outside the muffin-tin spheres, and so one may suggest that this is a better method for the treatment of the interstitial region. However, in this approach the spin moments in the interstitial region for the FM and AFM structures are treated differently: for the FM structure the spin moment is non-zero whereas for the antiferromagnetic state the moment of the interstitial is zero (although the spin density may of course be non-zero in this region).

The total magnetic moment per site as a function of volume is illustrated, using data obtained using the LSDA and PBE functionals within LMTO-ASA method, in figures 7 and 8 respectively. From these figures it is clear that the total magnetic moment increases as a function of volume for all magnetic structures. Indeed for the AFM structures the magnetic moment has a maximum of $\approx$7.25 μ_B which occurs at a volume of $1.04V_0$ and $1.11V_0$ for AFM_I and AFM_{II} respectively. It may also be noted that the magnetic moment per site for the FM structure is always larger than that for the AFM structure for all volumes greater than $0.75V_0$ and $0.78V_0$ if calculated using the LSDA or the PBE functional respectively. From these

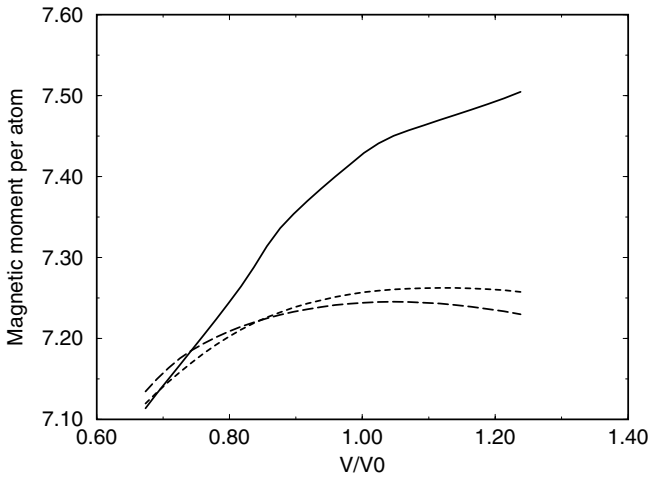

Figure 7. Magnetic moment as a function of V/V_0 for FM (solid line), AFM_I (dotted line) and AFM_{II} (dashed line) structures calculated using the LSDA functional within the LMTO-ASA method.

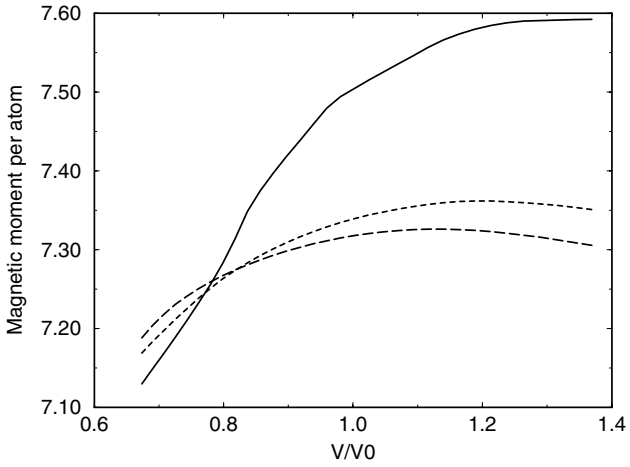

Figure 8. Magnetic moment as a function of V/V_0 for FM (solid line), AFM_I (dotted line) and AFM_{II} (dashed line) structures calculated using the PBE functional within the LMTO-ASA method.

figures it is clear that there is a direct correlation between the difference in magnetic moment for an atom in the FM structure and for an atom in the AFM_I structure ($\delta m = m_{FM} - m_{AFM}$) and the difference in total energy between these two magnetic structures ($\delta E = -(E_{FM} - E_{AFM})$). Our calculations determine that a crossover from AFM to FM occurs at δm in excess of 0.17 μ_B or 0.22 μ_B if calculated using the LSDA and PBE functional respectively. This crossover is also dependent on the method of calculation (ASA versus FP) and hence it is clear that the treatment of the magnetism within the interstitial region and the description of the exchange–correlation energy in the functional play a significant role in the description of the magnetic coupling between successive layers within bulk Gd.

It must also be noted that in the study of Gd using the FP-LMTO method presented in reference [11], placing the 4f electrons in the core rather than the valence region (as in this study) resulted in the predicted magnetic ground state being FM, regardless of the functional used in the calculation, with an equilibrium volume of $0.98V_0$ or $1.04V_0$ calculated using the LSDA or PBE functional respectively. Unfortunately it is difficult to compare the total energies of Gd using the 4f states as localized or delocalized, simply due to the fact that if the f states are localized, one must exclude the 4f basis functions in the expansion of the conduction electron states, and hence a comparison between the two calculations involves a comparison of total energies obtained from calculations with different basis sets, an uncertain procedure. Moreover, in both LSDA and PW91 calculations, the magnetic moment per site was found to be 7.75 μ_B—which is slightly larger than the experimental value given by reference [38].

In conclusion it can be stated that the correct magnetic ground state can be obtained, with an equilibrium volume close to experiment, if one uses the GGA within the LMTO-ASA method and the 4f electrons in the valence band. Alternatively, on the basis of the conclusions of [11] one may get the correct ground state, again with an equilibrium volume close to the experimental value, using the LSDA if the 4f states are treated as in the core states. However, it must be noted that the LMTO-ASA has a tendency to underestimate the magnetic moment per atom by an amount similar to that by which the FP-LMTO method overestimates it. Moreover some doubt can be cast on whether it is consistent to compare the total energy of the AFM Gd with that of FM Gd using the FP-LMTO method, as the spin density within the interstitial region is not treated in a consistent manner in the two calculations.

3.2. At various c/a ratios

The LMTO-ASA method was used to calculate the total energy as a function of volume for Gd in the FM, AFM_I and AFM_{II} structures. From these calculations it became apparent that the equilibrium volume of the unit cell is not dependent on the c/a ratio for all magnetic structures considered here. However, it was found that the difference in total energy between the FM and AFM_I magnetic structures is closely related to the c/a ratio.

Optimization of the c/a ratio has proved to be beyond the capabilities of the ASA due to the approximations made in the treatment of the potential (figure 9). Indeed it has been shown that optimizing this parameter is problematic even in a FP-LAPW approach due to the softness of Gd [5]. Use of the FP-LMTO method is a feasible approach to the problem—and indeed it may be noted that, for a fixed volume of V_0, a value of $c/a = 1.604$ is predicted for the FM structure regardless of whether the LSDA or PBE functional is used in the calculation (see figures 10 and 11). This is slightly larger than the experimental value and may be volume dependent, as the FP-LMTO method suggests that the equilibrium c/a for bulk Dy is strongly dependent on the volume of the unit cell [39].

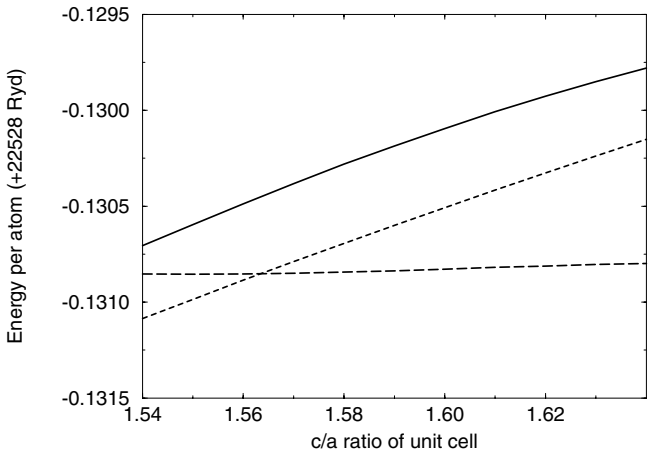

Figure 9. The total energy for FM, AFM_I and AFM_{II} ordered bulk hcp gadolinium for various interlayer spacings calculated at fixed volume V_0. The full line corresponds to the FM structure, the dashed line to the AFM_I structure and the dotted line to the AFM_{II} structure. All calculations were done using the LSDA functional.

The difference in total energy of an atom in FM ordered Gd and an atom in AFM ordered Gd is shown, as a function of the c/a ratio, in figures 12 and 13 calculated using the LMTO-ASA method and FP-LMTO method respectively. From both figures one can see that the use of the LSDA functional within either LMTO method will not predict a ferromagnetic ground state—unless the unit cell is subjected to considerable compression along the c-axis. Indeed use of the PBE functional within the LMTO-ASA method does shift this crossover from antiferromagnetism to ferromagnetism at a c/a ratio that is within +0.1% of the experimental value, with a tendency towards ferromagnetism for all c/a below this value. Conversely the crossover from AFM to FM behaviour is predicted to occur at smaller c/a if one uses a GGA instead of the LSDA functional within the FP-LMTO method.

In conclusion, it is evident that use of the PBE functional within the LMTO-ASA method does result in the prediction of the experimentally observed ferromagnetic structure for c/a within the specified range of $c/a < c_0/a_0 + 0.2\%$. For all c/a above this value the PBE

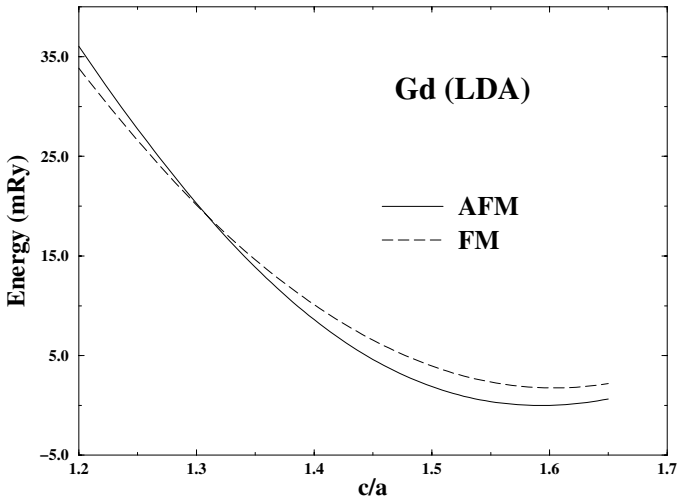

Figure 10. Total energy as a function of c/a ratio for FM (full line) and AFM (dashed line) structured Gd using the LSDA functional within the FP-LMTO method. The 4f electrons were treated as delocalized.

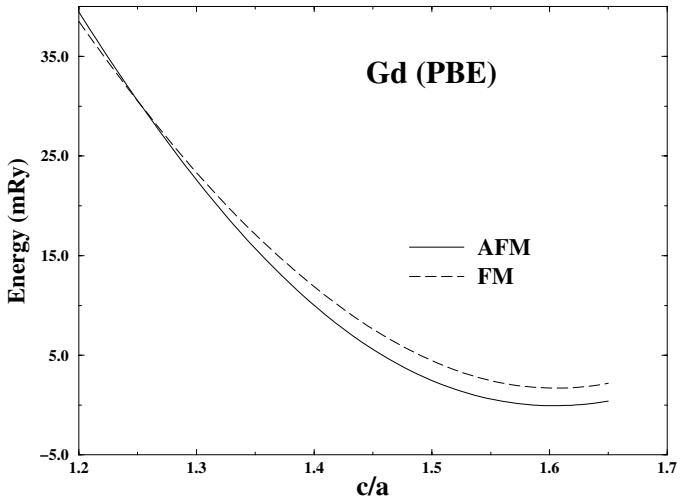

Figure 11. Total energy as a function of c/a ratio for FM (full line) and AFM (dashed line) structured Gd using the PBE functional within the FP-LMTO method. The 4f electrons were treated as delocalized.

functional predicts that the AFM_I structure is energetically preferable. This discovery that a small change in c/a can invoke a change in preferred interlayer magnetic coupling is anticipated to have significant consequences in the description of the nature of the magnetic coupling between the Gd(0001) surface and the underlying bulk. Finally the tendency for the LSDA functional to always predict antiferromagnetic coupling between successive layers within the bulk material can be directly related to the fact that early theoretical work, which used the LSDA functional, always predicted the magnetic coupling at the Gd(0001) surface to be antiferromagnetic—especially if the surface layer was relaxed outwards.

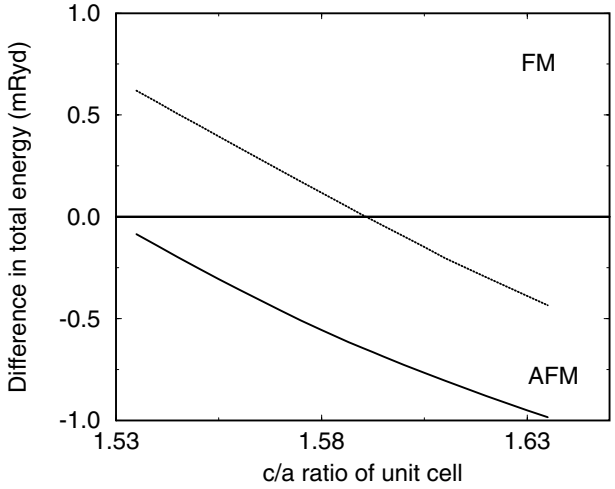

Figure 12. Difference in total energy between antiferromagnetically and ferromagnetically ordered bulk hcp gadolinium as a function of c/a ratio calculated at the experimental volume V_0 of 32.65 Å^3. The full line (bottom) was calculated using the LSDA and the dashed line (top) using the PBE functional.

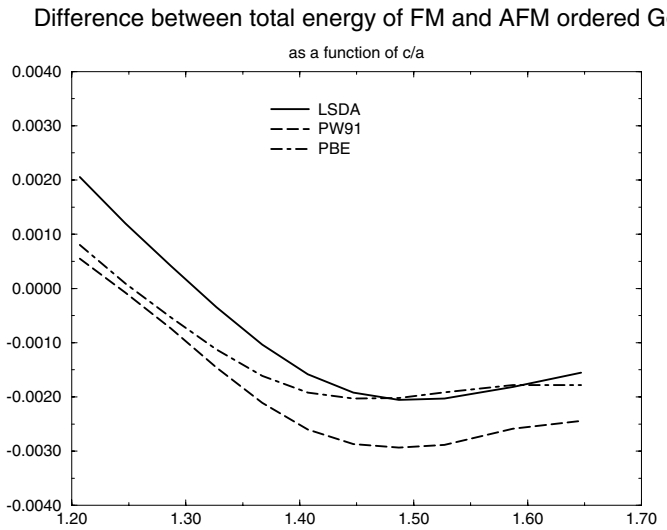

Figure 13. Difference in total energy as a function of c/a ratio between FM and AFM structured Gd calculated using the LSDA (full line), PW91 (dashed line) and PBE (dot–dashed line) functionals within the FP-LMTO method.

3.3. Magnetic coupling of the surface layer

The magnetic coupling of the Gd(0001) surface with the underlying bulk is modelled here using the approach described in section 2 and the supercell structures illustrated in figure 2. Using the PBE functional within the LMTO-ASA method the total energy as a function of relaxation of the surface layer was calculated for both AFM and FM coupling of the surface. Consideration of the difference in total energy between the two structures, as shown in figure 14, indicates that ferromagnetic coupling of the Gd(0001) surface to the underlying bulk is energetically

preferable at the experimental lattice parameters. Moreover if the surface layer is relaxed outwards by more than 6%, then the preferred magnetic coupling between this surface and the bulk material becomes antiferromagnetic. Evidently the crossover from AFM to FM coupling is strongly dependent on the effective c/a of the surface layer.

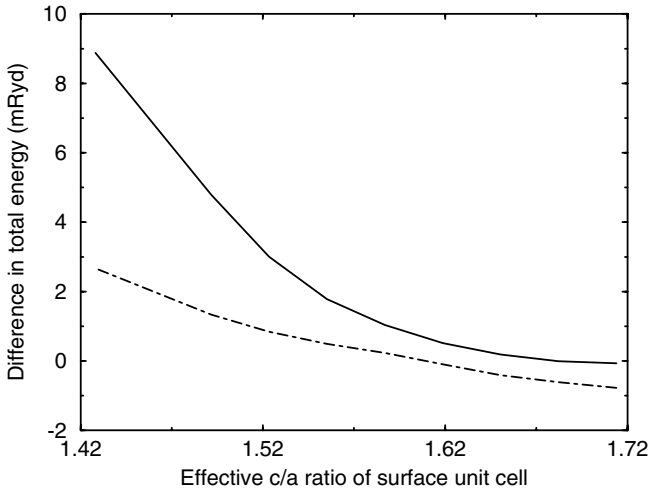

Figure 14. Difference in total energy and surface energy, as a function of c/a ratio *at the outermost layer*, for a slab with ferromagnetic/antiferromagnetic coupling at the surface/subsurface layer. The dot–dashed line indicates the energy difference for the surface layer in the two structures and the full line indicates the total difference in energy of the two slabs. All calculations were done using the PBE functional.

Decomposition of the total energy into its contributions from each layer in the supercell indicates that the magnetic preference of the outer layer as a function of effective c/a is similar to that of the bulk material and this can be clearly seen by comparison of figures 14 and 12 for the Gd surface layer and Gd bulk. Consequently it becomes evident that one can link the magnetic behaviour of this surface layer with the magnetic behaviour of the bulk material. In particular one can state that there is a relationship between compression along the c-axis with the tendency towards FM behaviour and expansion along the c-axis with the tendency towards AFM behaviour. For the bulk material it was found, and discussed in detail in the previous sections, that the crossover from AFM to FM behaviour was dependent on the functional and method used in the calculation. Consequently it is not surprising that the early theoretical work predicted an AFM coupling at the surface as preferable due to the fact that the magnetic ground state of the bulk material was predicted to be also AFM.

4. Conclusions

It is evident that the gradient correction of PBE within the LMTO-ASA can be used to obtain the experimentally observed ferromagnetic ground state of bulk hcp gadolinium. Moreover, use of this functional to describe the magnetic coupling of the Gd(0001) surface to the underlying FM bulk is also successful, as ferromagnetic coupling is predicted at the experimental lattice parameters. Indeed FM coupling is predicted to be energetically preferable for relaxations smaller than a 6% outwards movement of the outer surface layer. However, the prediction of the equilibrium relaxation of the surface layer is beyond the capabilities of the LMTO-ASA method.

The FP-LMTO method predicts an AFM ground state for bulk Gd regardless of whether or not a GGA is used, if the 4f electrons are treated as delocalized. Further examination of the total energy as a function of c/a also indicates that AFM coupling is energetically preferred—unless there is sufficient compression along the c-axis. Consequently it was not sensible to proceed to look at the magnetic coupling of the Gd(0001) surface using this method with delocalized 4f states.

Finally, recent work of Shick *et al* [40] also confirms an increasing tendency towards ferromagnetism on reducing the interlayer distance at the surface. In agreement with the present work, the origin of this effect is electron correlations and therefore it comes as no surprise that this large enhancement of the magnetic coupling as a function of interlayer separation is seen both in the bulk and at the surface.

Acknowledgments

This work has benefited from collaborations within, and has been partially funded by, the Training and Mobility Network on 'Interface Magnetism' and 'Electronic Structure Calculations of Materials Properties and Processes for Industry and Basic Sciences'.

References

[1] Heinemann M and Temmerman W M 1994 *Surf. Sci.* **307–309** 1121
[2] Heinemann M and Temmerman W M 1994 *Phys. Rev.* B **49** 4348
[3] Bylander D M and Kleinmann L 1994 *Phys. Rev.* B **49** 1608
[4] Bylander D M and Kleinmann L 1994 *Phys. Rev.* B **50** 1363
[5] Singh D J 1991 *Phys. Rev.* B **44** 7451
[6] Wang C S, Klein B M and Krakauer H 1985 *Phys. Rev. Lett.* **54** 1852
[7] Bagno P, Jepsen O and Gunnarsson O 1989 *Phys. Rev.* B **40** 1997
[8] Sticht J and Kubler J 1985 *Solid State Commun.* **53** 529
[9] Ahuja R, Auluck S, Johansson B and Brooks M S 1994 *Phys. Rev.* B **50** 5147
[10] Wu Ruqian, Li Chun, Freeman A J and Fu C L 1991 *Phys. Rev.* B **44** 9400
[11] Eriksson O, Ahuja R, Ormeci A, Trygg J, Hjortstam O, Soderlind P, Johansson B and Wills J M 1995 *Phys. Rev.* B **42** 4420
[12] Dowben P A, McIlroy D N and Li D 1997 *Handbook on the Physics and Chemistry of Rare Earths* vol 24 (Amsterdam: Elsevier Science) ch 159
[13] Temmerman W M, Szotek Z, Jenkins A C, Svane A, Winter H, Beiden S V and Gehring G H 1998 *Magnetism and Electronic Correlations in Local-Moment Systems: Rare-Earth Elements and Compounds* (Singapore: World Scientific) p 21
[14] Wu Ruqian and Freeman A J 1991 *J. Magn. Magn. Mater.* **99** 81
[15] Quinn J, Li Y S, Jona F and Fort D 1992 *Phys. Rev.* B **46** 9694
[16] Weller D, Alvarado S F, Gudat W, Schroder K and Campagna M 1985 *Phys. Rev. Lett.* **54** 1555
[17] Mulhollan G A, Garrison K and Erskine J L 1992 *Phys. Rev. Lett.* **69** 3240
[18] Starke K, Nava E, Baumgarten L and Kaindl G 1993 *Phys. Rev.* B **48** 1329
[19] Tang H, Weller D, Walker T G, Scott J C, Chappert C, Hopster H, Pang A W, Dessau D S and Pappas D P 1993 *Phys. Rev. Lett.* **71** 444
[20] Bylander D M and Kleinmann L 1994 *Phys. Rev.* B **50** 4996
[21] Pang A W, Berger A and Hopster H 1994 *Phys. Rev.* B **50** 6457
[22] Popov A P and Pappas D P 1997 *Phys. Rev.* B **56** 3222
[23] Li Dongqi, Pearson J, Bader S D, McIlroy D N, Walfried C and Dowben P A 1995 *Phys. Rev.* B **51** 13 895
[24] Weschke E, Schüssler-Langeheine C, Meier R, Fedorov A V, Starke K, Hübinger F and Kaindl G 1996 *Phys. Rev. Lett.* **77** 3415
[25] Donath M, Gubanka B and Passek F 1996 *Phys. Rev. Lett.* **77** 5138
[26] Krier G, Jepsen O, Burkhardt A and Andersen O K 1994 unpublished
[27] Wills J M and Cooper B R 1987 *Phys. Rev.* B **36** 3809
[28] Price D L and Cooper B R 1989 *Phys. Rev.* B **39** 4945

[29] von Barth U and Hedin L 1972 *J. Phys. C: Solid State Phys.* **5** 2064
[30] Perdew J P, Burke K and Ernzerhof M 1996 *Phys. Rev. Lett.* **77** 3865
[31] Chadi D J and Cohen M L 1973 *Phys. Rev.* B **8** 5747
[32] Froyen S 1989 *Phys. Rev.* B **39** 3168
[33] Perdew J P and Wang Yue 1992 *Phys. Rev.* B **45** 13 244
[34] Perdew J P 1992 *Phys. Rev.* B **46** 6671
[35] Temmerman W M and Sterne P A 1990 *J. Phys.: Condens. Matter* **2** 5529
[36] Langreth D C and Mehl M J 1983 *Phys. Rev.* B **28** 1809
[37] Hu C D and Langreth D C 1985 *Phys. Scr.* **32** 391
[38] Roeland L W, Cock G J, Muller F A, Moleman A C, Jordan R G and McEwan K A 1975 *J. Phys. F: Met. Phys.* **5** L233
[39] Fast L 1999 Private communication
[40] Shick A B, Pickett W E and Fadley C S 2000 *Phys. Rev.* B **61** R9213